International Journal of Biological Macromolecules 138 (2019) 590–601

Contents lists available at ScienceDirect

International Journal of Biological Macromolecules

journal homepage: http://www.elsevier.com/locate/ijbiomac

Sprayable and injectable visible-light Kappa-carrageenan hydrogel for in-situ soft tissue engineering

Shima Tavakoli, Mahshid Kharaziha *, Ahmad Kermanpur, Hamidreza Mokhtari

Department of Materials Engineering, Isfahan University of Technology, Isfahan 84156-83111, Iran

ARTICLE INFO

Article history:
Received 22 April 2019
Received in revised form 24 June 2019
Accepted 21 July 2019
Available online 22 July 2019

Keywords:
Kappa-carrageenan
Sprayable hydrogel
Injectability
Visible-light cross-linking

ABSTRACT

The aim of this study was to develop injectable and sprayable visible-light crosslinked Kappa-carrageenan (κCA) hydrogel and to investigate the role of polymer concentration (2, 4 and 6 wt%) and degree of methacrylation (6 and 12%) on its properties. It was found that, the average pore sizes, water content and swelling ratio of hydrogel were tunable by changing the methacrylate κCA (KaMA) concentration and methacrylation degree. Furthermore, the mechanical properties of KaMA could be noticeably modulated, depending on the formulation of hydrogel. Tensile and comprehensive modules were enhanced from 68 to 357 kPa and from 213 to 357 kPa, respectively, by increasing KaMA concentration from 2 to 6 wt% and methacrylation degree from 6 to 12%. Furthermore, with increasing methacrylation degree and polymer content, the absorbed energy and energy loss were increased. Moreover, recovery significantly enhanced from 27.3% to 74.4% with increasing polymer content from 2 to 6 wt%. Finally, visible-light crosslinked KaMA hydrogels not only was biocompatible, but also could promote HaLa cell and fibloblasts function. The visible-light crosslinked KaMA is thought to be an exclusive biomaterial as a sprayable hydrogel being able to cover skin injuries or to inject as a bio-printing material to in situ heal soft tissue damages.

1. Introduction

Recently, hydrogel-based constructs have been widely employed for the regeneration of soft tissues such as skin, blood vessel, muscle and fat [1,2]. Hydrogels are three-dimensional biocompatible and biomimetic structures which could encapsulate therapeutic agents, cells and biomacromolecules such as proteins, nucleotides, and peptides [3,4]. Between them, injectable and sprayable hydrogels transmute hydrogels to the unique biomaterials for suture-less closure of wounds, bioprinting and in-situ soft tissue reconstruction applications [5–7]. In-situ forming gels reveal various advantages consisting of invasive treatment reduction, ease of use, simple cell embedding and cost reduction [8]. In-situ forming hydrogels are synthesized by using different physical and chemical crosslinking strategies such as photo-crosslinking, thermo-crosslinking and ionic-crosslinking [9,10]. Many researches have been conducted in using non-toxic chemical photo-initiators to crosslink the hydrogels under ultraviolet (UV) light [7,10]. However, UV light has some drawbacks in tissue engineering applications such as DNA damage, immunosuppression, cell death, accelerating tissue aging and cancer induction [11]. These issues motivated researchers to use a safer wavelength of light like visible lights [11,12]. Visible light could reduce the DNA damages and increase cell viability chance [13,14]. Additionally, visible light could penetrate in the depth of tissues with lower energy than UV light. Thereafter, visible light crosslinkable hydrogels are appropriate choices to develop injectable and sprayable materials for tissue engineering applications.

The limited types of visible-light crosslinked hydrogels based on natural (e.g. polysaccharides and gelatin methacryloyl [15]) and synthetic (e.g. poly(ethylene glycol) diacrylate [16]) polymers and their combinations have been developed. In a study, Smeds and Grinstaff [15] synthesized in-situ photocrosslinkable methacrylated alginate (AA-MA) and methacrylated hyaluronan (HA-MA) hydrogel using Eosin Y and triethanolamine (TEA) as the photoinitiator and co-initiator, respectively, via 30 s argon ion laser exposure. In another study, Noshadi et al. [17] synthesized visible-light crosslinked gelatin methacryloyl (GelMA) hydrogels using Eosin Y, TEA and N-vinylcaprolactam (VC) as photoinitiator, co-initiator and co-monomer, respectively. The results proved the cytocompatibility of gel both in vitro and in vivo. Moreover, they revealed that different concentrations of TEA could influence mechanical strength, dramatically. In another study, Annabi et al. [11] utilized GelMA and methacryloyl-substituted recombinant human tropoelastin (MeTro) in order to fabricate a sprayable composite MeTro/GelMA hydrogels through visible light-mediated crosslinking for wound dressing applications. They found that as-prepared spray promoted healing of wounds with no harmful side effects.

Kappa-carrageenan (κCA), a natural linear water-soluble polysaccharide with one sulfated group per disaccharide (25 to 30% ester

* Corresponding author.
E-mail address: kharaziha@cc.iut.ac.ir (M. Kharaziha).

https://doi.org/10.1016/j.ijbiomac.2019.07.126
0141-8130/

sulfate content), is one of the appropriate biopolymer in tissue engineering. κCA mimics biomimetic property and resembles the natural glycosaminoglycan structures [18–21]. Mihaila et al. [10] synthesized a dual-crosslinkable hydrogel based on κCA for tissue engineering applications by using potassium ions and UV exposure. They employed κCA methacryloyl (KaMA) with different methacrylation degrees (low, medium and high) and revealed the formation of hydrogels with different mechanical properties depending on the methacrylation degree. However, the mechanical properties and injectability of KaMa were not satisfied. In order to overcome these issues, various researches based on nanocomposite hydrogels consisting of various types of nanoparticles (e.g. Nanosilicates [18], ZnO, CuO [22], silver [23], gold [24] and magnetic nanoparticles [25]) have been developed. For instance, we recently synthesized nanocomposite hydrogels based on KaMA-graphene oxide and found the significantly improved mechanical properties and injectability of KaMA hydrogel [26]. All of these nanocomposite hydrogels were synthesized based on UV-crosslinking process and did not reveal any sprayable properties. Moreover, they consisted of the secondary components to provide injectability. According to the author's knowledge, sprayable κCA hydrogel via visible-light crosslinking process with no harmful side effects has not been reported yet.

In this study, a sprayable and injectable hydrogel based on visible-light crosslinked κCA is synthesized. In this regard, after synthesis of KaMA with various methacrylation degrees (6 and 12% (v/v)), Eosin Y, TEA and VC are applied to develop visible light-mediated photocrosslinking hydrogel system for soft tissue engineering. Moreover, the role of various methacrylation degrees as well as various concentrations of KaMA (2, 4 and 6 wt%) on the physical, mechanical and biological properties of visible-light crosslinked KaMA are investigated. Finally, the spray-ability and injectability of visible-light crosslinked KaMA are investigated.

2. Materials and methods

2.1. Materials

Kappa-Carrageenan (κCA), a linear polysaccharide made of repetitive 1,3-linked β-D-galactopyranose and 1,4-linked 3,6-anhydro-D-galactopyranose segments ($M_W = 3 \times 10^5$ g/mol), was obtained from Sigma-Aldrich (22048). The 3,6-AnGal/Gal ratio was reported about 1:1.03. Moreover, methacrylic anhydride (MA) ($C_8H_{10}O_3$) (Sigma-Aldrich, 64100) and sodium hydroxide (NaOH, Merck Co) were supplied to synthesis KaMA. Photoinitiator Eosin Y (C_{20} H_8 Br_4 O_5) (Sigma-Aldrich, 230251), co-initiator triethanolamine (TEA) ($N(CH_2CH_2OH)_3$, Merck), co-monomer N-vinylcaprolactam (VC) (C_8 $H_{13}NO$) (Sigma-Aldrich, 415464) and potassium chloride (KCl, Merck) were purchased to fabricate visible-light crosslinked KaMA. In addition, Irgacure D-2959 (2-Hydroxy-4′-(2-hydroxyethoxy)-2-methylpropiophenone) (Sigma) was purchased to prepare UV-crosslinked KaMA as control. Dialysis membranes with cut-off ~12–14 kDa was also purchased from Betagen Co, Iran. In addition, double distilled water (DDW) was applied in whole investigates.

2.2. Synthesis of visible-light crosslinked KaMA hydrogel

KaMA with two different degree of methacrylation (low methacrylation: 6% (v/v) and high methacrylation: 12% (v/v)) was primarily synthesized by following our previous work [26]. Briefly, 1 wt% κCA solution in 100 ml DDW was prepared at 50 °C to achieve a homogenous solution. Consequently, 6.4 and 13.6 ml MA was added to two different κCA solutions, separately, and homogenized at 50 °C. Then, 5 M NaOH solution was added drop-wise in order to control the pH value of solution to 8. The solution was subsequently dialyzed against DDW using dialysis membrane for 7 days at 4 °C to eliminate the unreacted MA. Finally, KaMA solution was lyophilized and subsequently was stored at −20 °C for further experiments.

To create visible-light crosslinked KaMA hydrogel, different concentrations of lyophilized KaMA (2, 4 and 6 wt%) with two degree of methacrylation were dissolved in DDW at 80 °C in oven. Consequently, 0.75 wt% TEA and 1.25 wt% VC were added to KaMA solution and the solution was mixed with 0.5 mM Eosin Y solution with volume ratio of 4:1. Consequently, 10 μl of final solution was injected on a glass coverslip and exposed under white LED light (100 $Mw.cm^{-2}$) for 180 s to change the hydrogel color from pink to white transparent. Finally, 5 wt% KCl solution was gently sprayed on the chemical crosslinked gel to initiate physical crosslinking. In order to compare visible-light mediated KaMA with UV crosslinked one, as control, a sample containing 4 wt% KaMA with high methacrylation degree was also prepared using Irgacure D-2959 as photoinitiator under UV exposure following our previous procedure [26].

2.3. Characterization of visible light crosslinked KaMA hydrogel

The chemical modification or methacrylation of κCA was studied by H NMR spectroscopy (Bruker Avance, 500 MHz). H NMR spectra of κCA and KaMA were provided in deuterium oxide (D_2O), and a frequency of 500 MHz. Furthermore, Fourier transform infrared spectroscopy (FTIR, Bruker tensor) was applied to evaluate the chemical composition of KaMA samples and characterization of dual-crosslinked hydrogel bonds. In addition, ultraviolet–visible spectroscopy at a range of 200–600 nm was employed to optimize initiator concentrations. For this purpose, primary solutions of initiators were diluted 10 times and their light absorbance was detected. Additionally, scanning electron microscopy (SEM, Philips) was employed to investigate the hydrogel microstructure. The samples were lyophilized for 24 h, before imaging. Consequently, they were gold coated to provide acceptable images. Furthermore, SEM images were applied to evaluate the average pore size of samples ($n = 40$) using ImageJ software.

2.4. Physiological stability assessment of visible-light crosslinked KaMA

The role of KaMA concentration and methacrylation degree on the equilibrium water content (EWC), mass swelling ratio (MSR) and degradation rate of hydrogels ($n = 3$) were investigated. The samples were lyophilized, weighted (W_1) and, consequently, soaked in phosphate buffer solution (PBS) at 37 °C for 1 h. Following being wiped off, the hydrogels were weighted (W_2) and the EWC and MSR were estimated, using Eqs. (1) and (2), respectively [10]:

$$EWC = \frac{(W_2 - W_1)}{W_2} \times 100 \quad (1)$$

$$MSR = \frac{W_2}{W_1} \times 100 \quad (2)$$

Moreover, in order to investigate the degradation rate of hydrogels ($n = 3$), the samples were lyophilized, weighed (W_1) and soaked in 5 ml PBS. After 3, 7 and 14 days of incubation at 37 °C, the samples were lyophilized and were subsequently weighed (W_2). Lastly, the weight loss of samples was considered regarding to Eq. (3) [18]:

$$Weight\ loss\ (\%) = \frac{(W_1 - W_2)}{W_1} \times 100 \quad (3)$$

2.5. Mechanical property evaluation of visible-light crosslinked KaMA hydrogel

Hydrogels ($n = 3$) were injected in a cylinder mold with diameter of 11 mm and thickness of 5 mm and dual-crosslinked via light exposure

and subsequently KCl solution. After 1 h immersing in PBS solution, the hydrogels were compacted by a tensile tester (Hounsfield H25KS) using a load cell capacity of 500 N. The strain rate was kept at 1 mm/min. Consequently, according to the stress-strain curves, compressive strength and modules as well as toughness were estimated. The cyclic compressive test was also performed at a rate of 0.5 mm/min as 1st complete loading-unloading cycle until 60% of strain. After 24 h soaking in PBS, 2nd comprehensive cycle was performed. The energy lost throughout the cycle was assessed via calculation of the area between the loading and unloading cycle. Lastly, the recovery of hydrogels was determined via comparison of 1st and 2nd loading curves, according to the Mokhtari et al. research [26].

In order to evaluate tensile properties, the hydrogels were injected in a rectangular mold (15 mm × 5 mm × 1 mm), crosslinked and incubated in PBS for 1 h. Consequently, the samples were placed on a piece of tape within tension grips of tensile tester (Hounsfield H25KS, United Kingdom) by a strain rate of 1 mm/min. In addition, elastic modulus was considered by finding the slope of the stress-strain curves in linear region.

2.6. Rheology evaluation of visible light crosslinked KaMA hydrogel

In order to study injectability and spray-ability of KaMA solution, rheological test was applied by a viscometer (HAAKE RV12). Initially, flow test was completed to estimate the viscosity of polymer solution while shear rate was changed from 0.01 to 100 1/s, at 37 °C. Consequently, to evaluate the exact gelation time, the viscosity of primary hydrogel solution was measured during white LED light exposure at the shear rate of 100 1/s. Moreover, in order to clarify injectability of gel, the primary KaMA hydrogel was printed via an extrusion 3D bioprinting. Moreover, spray-ability was elucidated through spray the primary gel on a smooth substrate and the pictures are present.

2.7. Protein adsorption of visible light crosslinked KaMA hydrogel

The adsorption of bovine serum albumin (BSA) on the visible-light crosslinked KaMA hydrogels was investigated via batch contact method. Briefly, following 3 h soaking in PBS, the hydrogels ($n = 3$) were weighted and subsequently were soaked in 0.2 wt% BSA solution. To determine the residual BSA in solution, as-prepared supernatants were analyzed using UV–vis spectrophotometer at 289 nm. The amount of adsorbed protein (mg/ml) was considered based on Eq. (4) [27]:

$$\text{Adsorbed BSA (mg/g)} : \frac{C_0 - C_a}{W} V \tag{4}$$

In which C_0 and C_a are the concentrations of BSA (mg/ml) before and after adsorption, respectively. Moreover, W and V are the weight of swollen hydrogels (g) and the volume of BSA solution (ml), respectively.

2.8. Cell culture

HeLa and L929 Fibroblasts cell lines from National Cell Bank of Iran at the Pasteur Institute, were used to evaluate cellular behavior of KaMA hydrogels with different degree of methacrylation and polymer concentrations. Disk-like specimens with the thickness of 3 mm was prepared, rinsed with PBS (Bioidea, Iran), followed by sterilization in 70% ethanol and 3 h UV-exposure. Cells were incubated in Dulbecco's Modified Eagle Medium (DMEM, Gibco) supplemented with 10% (v/v) fetal bovine serum (FBS, Gibco) and 1% (v/v) streptomycin/penicillin (Gibco) at 37 °C under 5% CO_2. Finally, the cells with a density of 10,000 cells/well were seeded on the samples as well as tissue culture plate (TCP) (control) and were incubated at 37 °C under 5% CO_2 for 5 days.

Live/dead kit, supplied by Biotium, UK, was performed by HeLa cells according to the manufacturer protocol to study the role of hydrogel concentration and methacrylation degree on the viability of cells seeded on the hydrogels. In this regard, a staining solution consisting of ethidium homodimer (EthD-III) and calcein AM was added to the cell-seeded hydrogels, and incubated at 37 °C for 1 h. The dead and live cells stained with EthD-III and calcein-AM, respectively, were presented in red and green color under fluorescence microscopy, respectively. Finally, viability of HeLa cells was calculated by determining the percentage of green cells over total cell number. Moreover, in order to evaluate cell proliferation on the samples, 4, 6-diamidino-2-phenyl indole dihydrochloride (DAPI) staining was done. After 2 h fixation of the cell-seeded hydrogels by 4% (v/v) paraformaldehyde solution (Sigma Aldrich), the cells were permeabilized in 0.1% Triton X-100 (Sigma Aldrich). After washing with PBS, a 1:1000 dilution of DAPI solution (sigma-Aldrich, Germany) was added to samples to stain cell's nuclei. After 5 min soaking, the stained samples were considered using a fluorescence microscopy (Nikon TE 2000-U, Nikon instruments Inc., USA).

The relative survival of both cells (HeLa and fibroblasts) was also determined using MTT assay (Sigma Aldrich). After 1, 3 and 5 days of cell culture, the cell seeded samples and control were covered with MTT solution (0.5 g/ml). After 3 h incubation, the DMSO (Merck) was applied to dissolve the formazan crystals. Finally, the optical density (OD) of the dissolved formazan solution was estimated using a microplate reader (Biotek) against DMSO (blank) at 490 nm and finally the relative cell survival (% control) was estimated according to Eq. (5) [28]:

$$\text{Relative cell survival (\%control)} : \frac{X_{Sample} - X_b}{X_c - X_b} \tag{5}$$

where X_{Sample}, X_b and X_c are the absorbance of the sample, blank (DMSO) and control (TCP), respectively.

2.9. Statistical analysis

One-way ANOVA technique was utilized to analyze data. To establish a statistical significance between various sample groups, Tukey-Kramer post-hoc test was performed and P-value <0.05 was described as the statistical significant.

3. Results and discussion

3.1. Methacrylation of κCA

In this research, we proposed a new sprayable and injectable KaMA hydrogel to repair soft tissue damages. In this regard, κCA was methacrylated to synthesis KaMA with photo-polymerization potential (Fig. 1a). In addition, to verify successful methacrylation of κ-CA, H NMR (500 MHz) spectra were taken from KaMA with different methacrylation degree (Fig. 1b). In this research, we employed 6% (v/v) and 12% (v/v) methacrylic anhydride as low MA and high MA, respectively. In agreement with literature [29,30], H NMR spectrum of κCA comprised of the next chemical shifts: H NMR δ = 4.97 (H1), δ = 3.95–4.06 (H4), δ = 3.73–3.80 (H3), δ = 3.62 (H5, H6) and δ = 3.42 (H2). However, the spectrum of KaMA contained the methyl group (−CH_3) related peak and vinyl group (−CH=CH_2) double-peaks corresponded to the methacrylate groups at δ = 1.9–2 and 5.5–6 ppm, respectively. It could be concluded that the methacrylation of κCA at two different methacrylation degree (low-MA and high-MA) was performed. Furthermore, FTIR spectroscopy was applied in order to validate methacrylation procedure with different degrees. According to Fig. 1c, KaMA spectrum consisted of the characteristic peaks at 1530 cm^{-1}, 1620 $cm^{-1}$and 1730 cm^{-1} related to C—C, C═C and C═O, respectively. These peaks were not identified in the spectrum of κCA confirming the successful methacrylation process. Additionally, a slight shift could be detected at the position of the sulfate groups of κCA was (at 1215 cm^{-1} (O=S=O antisymmetric vibration) and

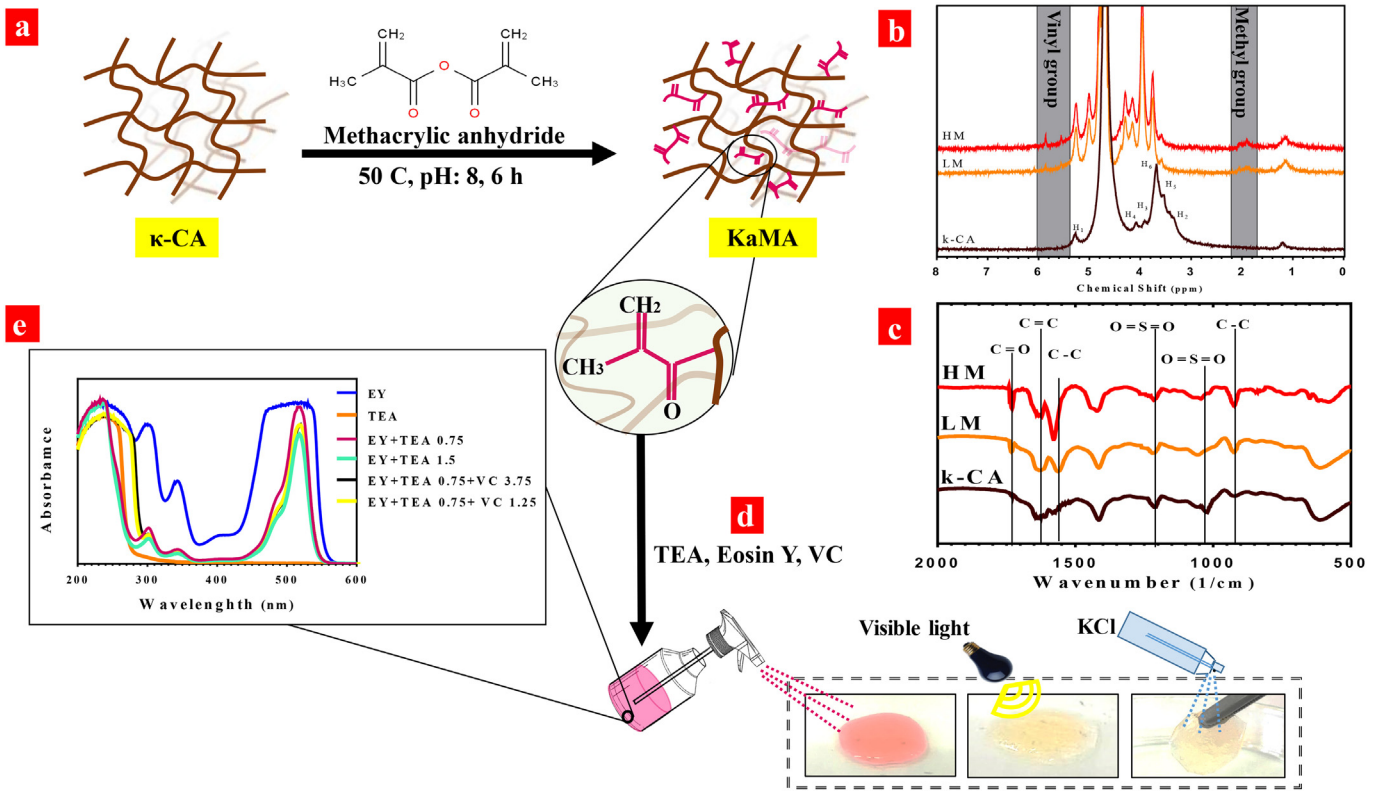

Fig. 1. Synthesis of visible-light crosslinkable KaMA hydrogel: a) the schematic representation the methacrylation of κCA, b) H NMR spectra and c) FTIR spectra of κCA and KaMA with different degree of methacrylation. d) Incorporation of photoinitiator, co-initiator and co-monomer to KaMA solution and consequently dual-crosslinking process under visible light exposure and KCl ions results in the formation of KaMA hydrogel. e) UV–vis spectra of different initiator ratios (EY: Eosin Y).

1023 cm^{-1} (O=S=O symmetric bond)) confirming that the sulfate group of κCA was not changed during the methacrylation process.

3.2. Structural characteristics of visible-light crosslinked KaMA hydrogel

In order to achieve a visible-light-mediated photo-crosslinking hydrogel, Eosin Y, TEA and VC were added to the initial polymeric solutions as a photo-initiator, co-initiator and co-monomer, respectively. Following the spraying the solutions on a substrate and exposing under white LED lamp for chemical crosslinking, KCl was sprayed gently as an ionic crosslinking agent (Fig. 1d). In order to optimize the concentration of photo-polymerization agent, light absorbance of photo-initiator, co-initiator and co-monomer with different ratios were characterized to minimize gelation time. According to Fig. 1e, while Eosin Y revealed a width absorbance peak at 450–550 nm, TEA did not have any absorbance under white light. Bahney et al. [16] similarly found that incorporation of TEA in Eosin Y aqueous solution not only restricted absorbance limitation but also reduced light absorbance with increasing the concentration of TEA from 0.75 wt% to 1.5 wt%. In another hand, in order to evaluate VC concentration on the gelation time, two various concentrations of VC (1.25 and 3.75 wt%) were added to the initiator solution (0.75 wt% TEA and 0.5 mM Eosin Y solution (volume ratio of 4:1)). Results revealed that although the incorporation of VC to the initiator solution reduced the maximum absorbance at 520 nm, the absorbance was not significantly changed in the presence of different concentrations of VC. Furthermore, color changing of two different primary hydrogel solutions was considered, separately. The time of color changing from pink to glassy was reduced from 240 to 180 s for 10 μl solution, when the VC concentration decreased from 3.75 wt% to 1.25 wt%. Therefore, 0.75 wt%, 1.25 wt% and 0.5 mM were selected as the optimized concentrations of TEA, VC and Eosin Y, respectively, for the next experiments.

After selection of the optimized components, the visible-light crosslinked KaMA hydrogel was prepared and characterized. According to the photos of hydrogel containing 4 wt% KaMA with low and high degree of methacrylation (Supplementary Fig. S1a), the color of hydrogel cylinders was changed to bright yellow after visible light exposure. Moreover, the appearance of hydrogels was independent with polymer concentration and methacrylation degree. In order to characterize dual-crosslinked hydrogels containing 4 wt% KaMA with low and high degree of methacrylation, FTIR spectroscopy was applied (Supplementary Fig. S1b). Both spectra consisted of vinyl (−CH=CH_2) and methyl (−CH_3) functional groups which are more intensive in the hydrogel with higher degree of methacrylation. The methacrylation functional groups are remarked with C—C, C=C and C=O bonds at 1550 cm^{-1}, 1620 $cm^{-1}$and 1720 cm^{-1} respectively, which are penetrate to each other as a result of chemical bonds formation after visible light exposure. Moreover, the vinyl peaks in both samples were stronger than vinyl peaks in the lyophilized KaMA spectrum, due to incorporation of VC as a co-monomer which promoted the chemical crosslinking efficiency. On the other hand, although all κCA characteristic peaks were presented in both spectra, their intensity was different, depending on the methacrylation degree. Results revealed that increasing methacrylation degree enhanced the interaction between κCA branches with functional methacrylation groups which decreased κCA characteristic peak intensity. Mihaila et al. [10] similarly studied dual crosslinked κCA with different degrees of methacrylation and found the reduced intensity of κCA characteristics peaks with increasing methacrylation degree of κCA. Moreover, as κCA undergo a transition of coil-helix conformation, gelation also occurred in the presence of KCl as an ionically crosslinking agent [18]. Our results revealed that the physical crosslinking density was higher in the hydrogels with lower methacrylation degree. With increasing methacrylation modification degree, the side chain interactions reduced leading to double helix configuration reduction [10].

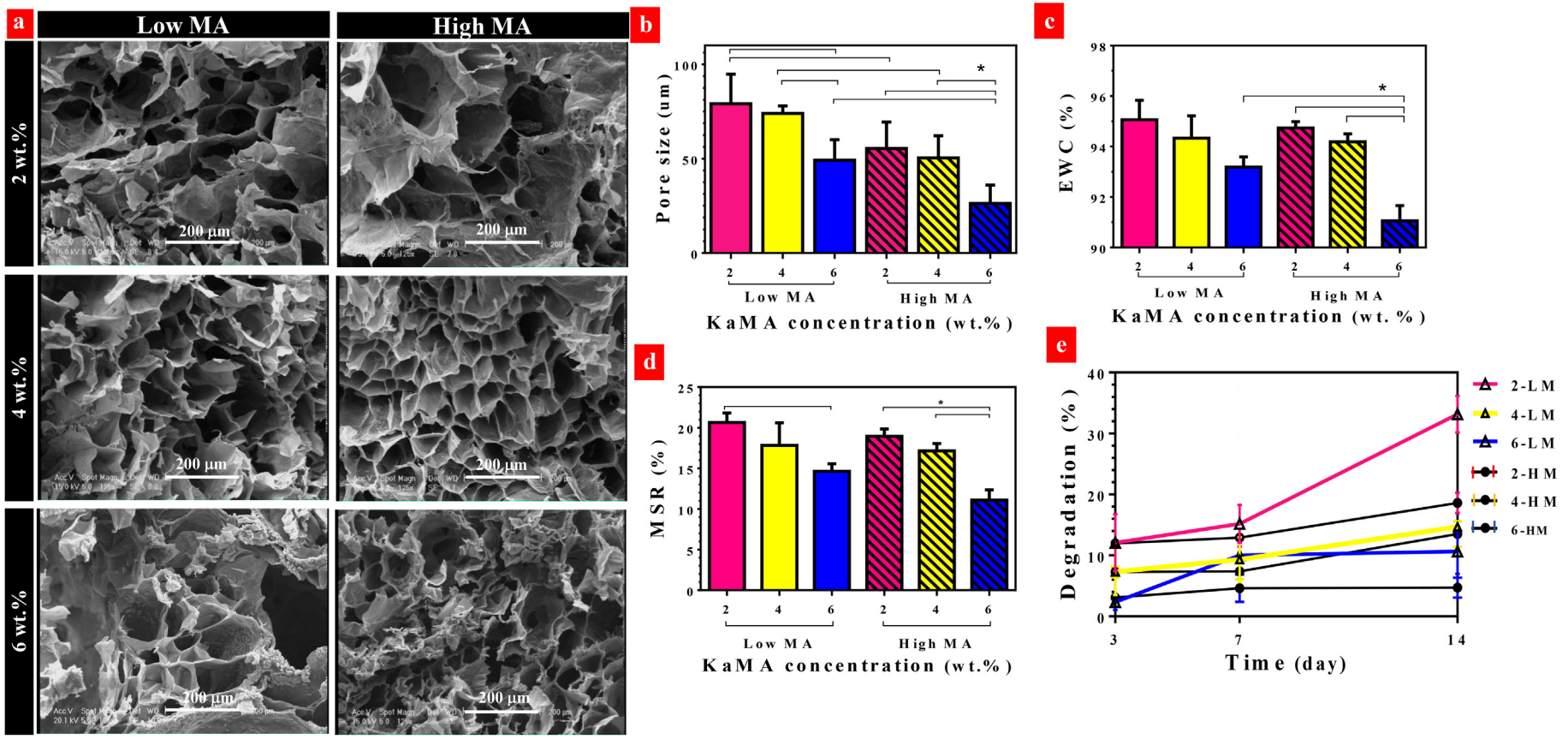

Fig. 2. Physical evaluation of visible-light crosslinkable KaMA hydrogel: a) SEM images of the 2-LM, 2-HM, 4-LM, 4-HM, 6-LM and 6-HM hydrogels. b) The average pore size of lyophilized hydrogels. c) EWC and d) MSR of KaMA hydrogels after 1 h drenching in PBS solution at 37 °C. e) The degradation of KaMA hydrogels during 14 days of incubation in PBS (*: $P < 0.05$).

SEM images of hydrogels containing various concentrations of KaMA precursors (2, 4 and 6 wt%) at two different low (2-LM, 4-LM and 6-LM, respectively) and high (2-HM, 4-HM and 6-HM) methacrylation degrees are presented in Fig. 2a. Results showed the clumping of the hydrogel and destruction of the structural organization with increasing KaMA concentration due to stronger chain linkages. This behavior was noticeable at the higher methacrylation degree of KaMA. Moreover, Fig. 2b revealed that the average pore size of the hydrogels decreased with rising methacrylation degree from 6% (low) to 12% (high). For instance, at 4 wt% KaMA sample, the average pore size reduced from 74 ± 3 μm to 49 ± 11 μm by increasing methacrylation degree. This behavior originated from higher chemical crosslinking density due to high methacrylation degree [10]. Similar result was reported by Guo et al. [31] on collagen/chondroitin sulfate/hyaluronan hydrogel who found that the porosity distribution and morphology order obstructed by increasing methacrylation degree due to a denser crosslinked structure. Furthermore, the effect of KaMA concentration on the wall widths and pore size was evaluated. Fig. 2b demonstrated that increasing KaMA content in hydrogel matrix resulted in the wall-widths thickening and shrinking pores. For example, the average pore size dropped from 79 ± 15 μm to 34 ± 3 μm by increasing KaMA content from 2 to 6 wt% in low methacrylation group. Moreover, in high methacrylation class, the average pore sizes stepped down from 55 ± 14 μm to 26 ± 10 μm by increasing KaMA concentration from 2 wt% to 6 wt%. Similarly, Shi et al. [32] found that with increasing polymer concentration in hydrogel matrix, polymer structure became denser. Higher polymer content network highly condensed polymer chains leading to diminished pore sizes in hydrogel network [32]. Porosity is an essential feature for hydrogel based scaffolds in tissue engineering to facilitate cell encapsulation and proliferation, vascularization, boost nutrients transportation and omit waste products [9,33]. For instance, in order to engineer unmineralized organic component of bone (osteoid), muscle and skin and tissues, the required porosity size are in the range of 40–100 μm, 50–100 μm and 25–40 μm, respectively [34–36]. Our results demonstrated that KaMA hydrogel could be applied for various tissue engineering applications, depending on the KaMA concentration and methacrylation degree.

Additionally, equilibrium water content (EWC) and mass swelling ratio (MSR) were determined after 1 h incubation in PBS at 37 °C (Fig. 2c–d). Our results indicated higher methacrylation degree caused lower mass swelling and water content in hydrogel. In addition, the presence of higher KaMA content in hydrogel matrix decreased mass swelling ratio and water content. For instance, EWC dropped from 95 ± 1% to 91 ± 1% by increasing KaMA concentration from 2-HM to 6-HM. It could be due to role of methacrylation degree and KaMA concentration on the crosslinking density and pore sizes (Fig. 2b). Similar results were reported by Nichol et al. [37] on GelMA hydrogels with different degree of methacrylation and polymer concentrations. Their results revealed the mass swelling of gels was dependent on the pore size. They found that higher methacrylation degree and more polymer concentration in a hydrogel network resulted in pore size reduction leading to less water molecule penetration in structure leading to lower EWC and MSR [10,37].

3.3. In vitro stability assessment of visible light crosslinked KaMA hydrogel

One of the fundamental characteristics of hydrogel is their controllable degradation in physiological environment. In order to investigate degradation behavior of KaMA in vitro, the samples were incubated in PBS at 37 °C for different time periods (3, 7 and 14 days). The degradation trends, during a 14-day period, are depicted in Fig. 2e. Results demonstrated that the degradation rate of all samples enhanced with increasing incubation time. However, between the samples, the highest KaMA concentration (6 wt%) resulted in a more stable hydrogel over a period. For instance, the 6-HM sample degraded <5% over the incubation period. Moreover, higher methacrylation degree resulted in reduced hydrogel degradation in PBS. Noticeably, degradation rate of 6-LM hydrogel significantly reduced from 10.6 ± 3.6% to 4.7 ± 1.6% with increasing the methacrylation degree. The denser and packed hydrogel networks could degrade and dissolute more slowly than hydrogels with wider pores due to less entrance of water molecules and swelling ratios [10]. A similar degradation trend was obtained by Mihaila et al. [10] based on UV-crosslinked KaMA hydrogels with different methacrylation degrees in PBS and DMEM environments.

3.4. Mechanical properties of visible light crosslinked KaMA hydrogel

Mechanical characteristics of hydrogels were studied through compression and tensile tests. According to Fig. 3a, the concentration of KaMA significantly affected the elastic modulus of hydrogel. For example, the elastic modulus of 2-HM and 2-LM samples increased 2.5 and 8-times, respectively, with increasing KaMA concentration to 6 wt% (6-HM and 6-LM, respectively). Annabi et al. [11] reported a similar trend for a sprayable MeTro/GelMA gel. They demonstrated that the elastic modulus significantly enhanced with increasing the MeTro/GelMA concentration from 15 to 20 wt%. However, the maximum elastic modulus of MeTro/GelMA gel was reported about 32 kPa, which was significantly less than that of the present research. On the other hand, we found that at the specific concentration of KaMA, the elastic modulus of KaMA hydrogel enhanced with increasing the methacrylation degree. This behavior was likely due to formation a firmer hydrogel matrix during polymerization by increasing chain aggregations and crosslinking density [11,37]. Moreover, the mechanical properties of visible-light crosslinking hydrogels applied for soft tissue engineering are crucial after spray on objective organ to avoid failure due to the mechanical mismatch. Our results demonstrated that the elastic modules of visible-light crosslinked KaMA was in the range of many soft tissues such as skin (80–300 kPa), liver (300–800 kPa) and tendon (30–50 kPa), confirming the potential of this sprayable and injectable hydrogel for soft tissue engineering [38,39].

Additionally, compression stress-strain test was performed until the sample failure. The samples were destroyed in 85–95% strain, depending on the methacrylation degree and polymer concentrations. The samples which have more KaMA concentration and higher methacrylation degree failed at higher strains. For instance, 6-HM sample was devastated at the 95% strain. The stress- strain curves of samples were also plotted until 60% strain (Fig. 3b). The inset Fig. 3b shows the stress-strain curves at the 5–15% strain region. According to the mechanical curves, the compressive strength and modulus as well as toughness were calculated (Fig. 3c–e). According to Fig. 3c, compressive strength of hydrogels was influenced dramatically by KaMA concentration and degree of methacrylation. For instance, the degree of methacrylation noticeably promoted compressive strength of KaMA hydrogel from 388 ± 11 kPa to 602 ± 19 kPa in 4-LM and 4-HM hydrogels, respectively. Moreover, at a constant methacrylation degree, the mechanical strength of KaMA enhanced with increasing the concentration of KaMA. For example, the compressive strength significantly enhanced from 114 ± 13 kPa (2-HM) to 900 ± 29 kPa (6-HM) when the concentration of KaMA enhanced from 2 to 6 wt% ($P < 0.05$). Similar result was discussed by Nichol et al. [37] on GelMA with three different methacrylation degree (low, medium and high) and polymer concentrations (5, 10 and 15 wt%). Moreover, compressive modulus was measured from the slop of compressive strain- stress curves through 5–15% strain (Fig. 3d). Results indicated that the compressive modulus of dual-crosslinked hydrogels was considerably improved with rising KaMA concentration and degree of methacrylation. Additionally, toughness was calculated from the compressive stress-strain curves (Fig. 3e). A similar trend was detected in toughness measurements. Results demonstrated that the highest toughness of KaMA hydrogel was obtained when the concentration of polymer and methacrylation degree were adjusted to 6 wt% and 12% (v/v) MA. Noticeably, at higher polymer concentrations, increasing methacrylation degree significantly enhanced

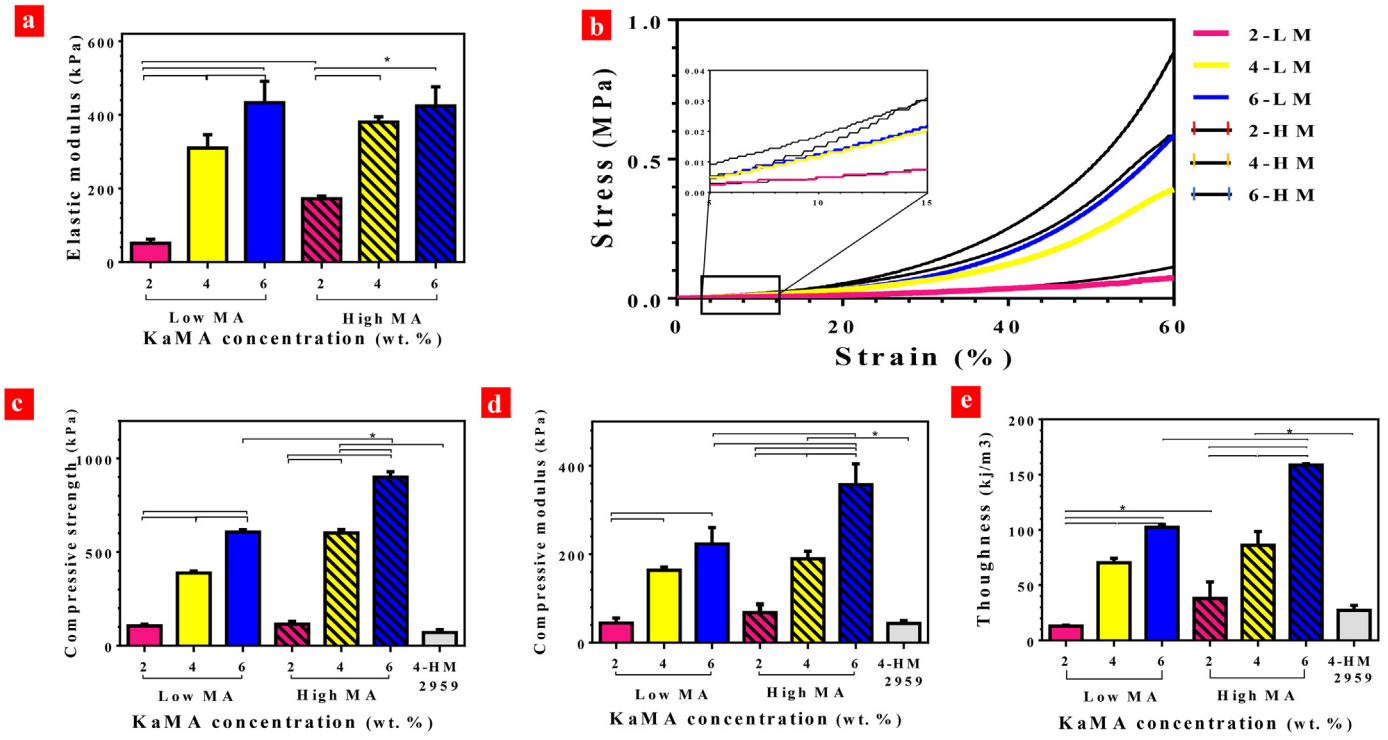

Fig. 3. Mechanical characteristics of visible-light crosslinkable KaMA hydrogel: a) elastic modulus of the 2-LM, 2-HM, 4-LM, 4-HM, 6-LM and 6-HM samples, b) the compressive stress-strain curves of samples, c) compressive strength (at 60% strain), d) compressive modulus and e) toughness of visible light-crosslinkable KMA hydrogels as well as UV-crosslinkable KaMA hydrogel. All values are described as corresponding to the averages ($n = 3$) ± standard deviation (*: $P < 0.05$).

compressive modulus and toughness. It could be due to stronger chemical crosslinking and deeper chain integration. Generally, photo-crosslinking potential of κCA provided via methacrylation process due to creation of vinyl ($-CH=CH_2$) and methyl ($-CH_3$) groups which are the photoinitiator targets. Therefore, the hydrogels with higher methacrylation degree are more likely to photo-crosslink under light exposure leading to a stronger gel network with smaller pore size [10,40]. Similarly, Mihaila et al. [10] found that the methacrylation degree and concentration of KaMA enhanced the crosslinking density leading to integration of polymer chains and consequently enhanced compressive modules. In addition, the mass swelling ratio is crucial in the mechanical properties of the hydrogels. The penetration of water molecules in the hydrogel structure resulted in the loosening the chain-chain interactions. Our results confirmed that the mechanical strength of the sprayable KaMA was significantly higher than previous ones. For instance, 12.5 wt% GelMA hydrogel provided compressive modulus in the range of 5–56.5 kPa depending on photo-initiator concentrations [17]. In another study, the modulus of MeTro/GelMA gel was considered about 60 kPa after exposure under visible light [11]. Accordingly, 6-HM sample has the highest elastic modulus, mechanical strength and toughness which cannot match with a wide range of soft tissue mechanical properties. On the other hand, the presence of 2 wt % KaMA in hydrogel structure could not provide enough mechanical stiffness for hydrogel network. Subsequently, 4-HM and 6-LM hydrogels which approximately have similar mechanical properties are more appropriate for different soft tissue engineering.

To evaluate the function of visible-light crosslinking method on the mechanical performance of KaMA hydrogel, a dual-crosslinked KaMA hydrogel synthesized via two-step UV crosslinking and consequently ionic crosslinking process. In this regard, the KaMA hydrogel containing 4 wt% KaMA with high methacrylation degree was UV crosslinked using Irgacure D-2959 as photo-initiator. In this regard, mechanical strength, compressive modulus and toughness were measured through compressive stress-strain test. As depicted in Fig. 3c, the compressive strength of ionic and UV-crosslinked KaMA hydrogel was approximately 9-times lower than 4-HM sample. In addition, the compressive modulus (Fig. 3d) and toughness (Fig. 3e) of KaMA dramatically decreased in UV mediated KaMA compared to those of 4-HM specimen. Similarly, Bahney et al. [16] confirmed that the poly(ethylene glycol) diacrylate (PEGDA) hydrogel fabricated by visible light polymerization had considerably higher chemical crosslinking density than PEGDA hydrogels formed by Irgacure D-2959 with UV light which led to the construction of a weaker hydrogel network under UV light exposure.

3.5. Viscoelastic behavior of visible light crosslinked KaMA hydrogel

To investigate the viscoelastic properties of the engineered hydrogels, cyclic compressive test with a maximum strain of 60% for 2 cycles were performed (Fig. 4a). Between 2 cycles, the specimens were soaked in PBS for 24 h. Subsequently, by plotting both first and second cycle loading, the recovery curve was discovered (Fig. 4a). Our results demonstrated that the strength of specimens enhanced with increasing polymer content and methacrylation degree, in both first and second cycles. However, strength of the samples in the second cycle was less than first one, which could be due to the breaking of some chemical bonds in the first cycle, while others stood out until 60% strain. However, with increasing methacrylation degree, these chemical bonds enhanced, leading to improved mechanical strength of high methacrylated series (2-HM, 4-HM and 6-HM) compared to that of the low methacrylated series (2-LM, 4-LM and 6-LM), at both first and second cycles. Furthermore, the number of unbroken chemical bonds enhanced with increasing polymer content, leading to superior strength at the second cycle. In another word, ionic crosslinking, based on K^+ ions and H-bonding along the primary carbohydrate structure of polymer, were dissipated part of energy by breaking these bonds [41]. Unlikely, part of ionic broken bonds was healed in PBS, leading to enhanced strength of samples at the second cycle. Moreover, the energy loss was calculated based on the area of loading and unloading and is presented in Fig. 4b. In the first cycle, with increasing methacrylation degree of hydrogel containing 2 wt% KaMA, the energy loss significantly

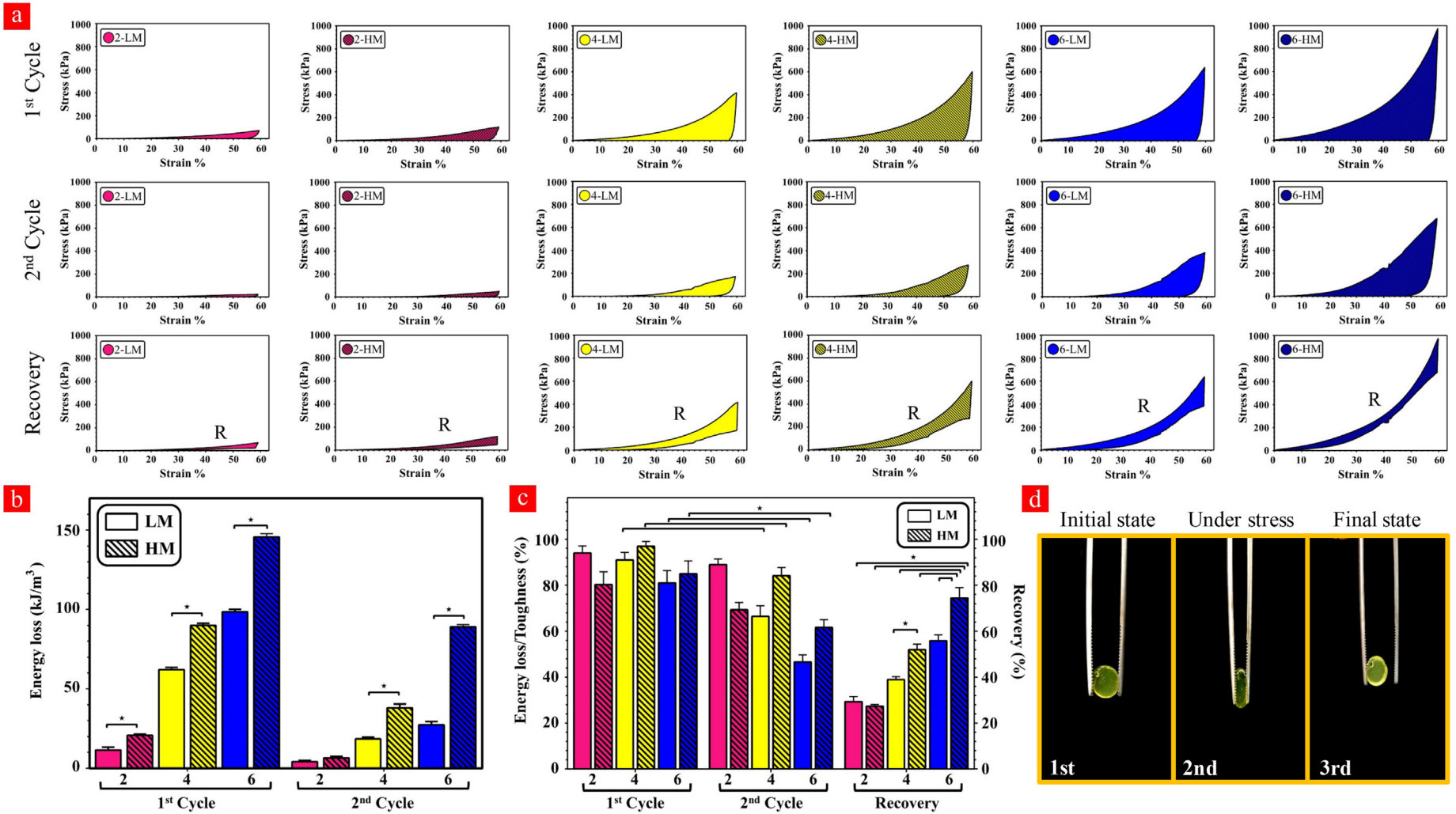

Fig. 4. Cyclic compression test for compressive properties of KaMA hydrogels: a) cyclic stress-strain curves of KaMA hydrogels. The hydrogels were compressed until 60% strain, preserved in PBS solution for 24 h and, subsequently, prepared for the second cycle. Recovery was estimated by comparison of area under the first and second loading curves by the cycle test, b) energy loss at the first and second loading cycles of hydrogels ($^*P < 0.05$). The energy loss during the cycles calculated by defining the area between loading and unloading cycles of curves, c) recovery and energy loss/toughness of hydrogel through cyclic tests ($^*P < 0.05$). d) The pictures showing the recovery properties of 4-HM hydrogel.

increased from 12 ± 1 kJ/m^3 (for 2-LM) to 21 ± 1 kJ/m^3 (for 2-HM). However, in the second cycle, the energy loss difference between 2-LM and 2-HM was not significant which might be due to the weak crosslinking process of 2 wt% hydrogel. At this sample, the majority of chemical bonds were broken leading to a similar behavior for 2-HM and 2-LM hydrogels. However, at the highest concentration of KaMA hydrogel (6 wt%), energy loss significantly increased from 99 ± 2 kJ/m^3 (for 6-LM) to 146 ± 2 kJ/m^3 (for 6-HM) with increasing methacrylation degree, in the first cycle. This significant increase was also detected in the second cycle. In another word, energy loss to toughness ratio was calculated for each specimen (Fig. 4c). While this ratio was not changed at less concentrations of KaMA (both 2-LM and 2-HM), it was significantly decreased from 81.7% (1st cycle) to 46.5% (2nd cycle) at 6-LM hydrogel. A significant decrease was also detected, between first and second cycle for 6-HM. Generally, all specimen was dual-crosslinked; chemical crosslinking by producing covalent bond and ionic crosslinking with intra- and inter-chain hydrogen bonds and interaction between SO_4^{-3} groups and K^+ ions. At lower polymer concentration (2-LM and 2-HM), after breaking of weak hydrogen bonding, the chemical bonds were broken dramatically by destructive strain. Consequently, after 24 h soaking in PBS, the predominant ionic re-crosslinking was enhanced while energy loss to toughness ratio was not significantly changed. However, at higher polymer concentration (6-LM and 6-HM), while ionic bonds were broken mostly, in the first cycle, the covalent bonds were not significantly affected. Therefore, the predominant covalent bonds played the main role and subsequently energy loss to toughness ratio was decreased, considerably. The recovery percentage of samples (Fig. 4c) was also accelerated with increasing polymer concentration for all specimens. The recovery significantly enhanced from 27.3% for 2-HM to 74.4% for 6-HM with increasing polymer concentration. Moreover, except 2-LM and 2-HM hydrogels, recovery of hydrogels considerably enhanced with increasing methacrylation degree. Recovery is usually a result of recreating some of broken bonds in the hydrogels developed with ionic crosslinking process. Fig. 4d shows that 6-HM hydrogel not only could recover its mechanical properties, but also could nearly recover its initial shape after 24 h immersing in PBS solution and following the severe strain. Mihaila et al. [10] similarly reached the dual-crosslinked hydrogels formed by Irgacure D-2959. Compared to our 6-HM hydrogels, the mechanical strength of Mihaila's hydrogel was 6.5 times lower than 6-HM, but its recovery in 2 cycles was 96.5%. In conclusion, with increasing methacrylation degree and polymer content, the absorbed energy (due to the mechanical stringent) and energy loss increased. Moreover, recovery significantly enhanced with increasing polymer content. Although recovery increased, with increasing methacrylation degree, in low polymer content, the significant change was not detected.

Effect of different photoinitiator (visible-light mediated crosslinker and UV-mediated crosslinker) on viscoelastic behavior was also evaluated (Supplementary Fig. S2). The results showed that energy loss in 4-HM was 7.5–times and 5–times greater than ionic and UV-crosslinked KaMA hydrogel, in first and second cycle, respectively. Our results demonstrated that visible-light crosslinked KaMA provided a stronger hydrogel network. However, the recovery increased from 52% to 66%, when the photoinitiator changed to Irgacure D-2959. It might be due to the more effective role of covalent bonds on the mechanical properties of 4-HM than UV-crosslinked one.

3.6. Rheological behavior of KaMA solution

Injectability and spray-ability of hydrogels are two distinctive characteristics which facilitate in-situ recruitment of damaged organs. In order to evaluate injectability and spray-ability of primary KaMA solutions containing photoinitiator, the 4-HM and 6-HM samples were analyzed due to their similar mechanical characteristics and proper physical property for soft tissue engineering. Fig. 5a revealed that the viscosity of primary KaMA solutions decreased with increasing shear rate. In this regard, the viscosity of 4-HM sample decreased from 3390.0 to 12.2 mPa.s, while in the case of 6-LM sample, the viscosity reduced from 17,123.1 to 257.3 mPa.s, once the shear rate boosted from 0.01 to 100 1/s. These trends illustrated the shear thinning behavior of KaMA solutions which could be appropriate for injection [26]. In addition, increasing the methacrylation degree resulted in the reduced primary solution viscosity over the shear rate period (0.01–100 1/s). It could be due to the role of enhanced methacrylation modification degree on the reduction of side chain interactions leading to reduced double helix configurations [10].

Injectable and sprayable visible-light mediated hydrogels are unique materials which could be easily in-situ applied in tissue engineering without any harmful side effect that associated with UV crosslinking systems. In this research, Eosin Y, TEA and VC were added to the KaMA solution as a photoinitiator, co-initiator and a co-monomer, respectively to encourage visible-light crosslinking process. The gelation time could be considered via measurement of the gel viscosity during different periods of UV radiation under white LED light. In this regard, the 4-HM and 6-LM samples were analyzed at the shear rate of 100 1/s. Fig. 5b revealed that there was a gelation point in both samples in which the viscosity jumped dramatically due to the additional polymerization mechanism. According to Fig. 5b, there was no significant difference in gelation time (90 s) of two samples. Although the degree of methacrylation was higher in the 4-HM sample, the higher concentration of KaMA content in 6-LM hydrogel resulted in reduced gelation time to that of 4-HM sample. According to Fig. 5c, in this mechanism, the crosslinking process was performed via free radical addition reactions from unsaturated monomers. At a distinguished point, the polymer chains terminate by joining to each other leading to gelation. Moreover, the visible light stimulates Eosin Y from the zero state to triple, which abstracts hydrogen atoms from TEA. Consequently, the deprotonated TEA radicals trigger the radical point formation in the methacryloyl groups of KaMA hydrogels. In addition, the presence VC enhances the vinyl group concentration and the number of radicals, during visible-light gelation leading to enhanced gel formation rate [11,17]. Based on this gel formation process, increasing methacrylation degree enhanced the formation of radical target groups which accelerated the gelation time. On the other hand, polymer concentration also influenced gelation time. Presence of more polymer content in a distinguished hydrogel volume reduced gelation time due to the presence of more groups for photo-reactions, as similarly reported in previous researches [42,43]. In another word, spray-ability of hydrogels could be facilitated with lower viscosity of primary solution due to the reduction of droplet size after pumping spray [44]. Therefore, according to above results (Fig. 5a), it could be found that 4-HM sample could be a proper biomaterial for in-situ sprayable hydrogels to rapidly heal and repair injuries (Fig. 5d). In this regard, the adhesive strength of this hydrogel was evaluated through tensile test, according to ASTM F2255–05 standard and Kim et al. work [45], using cow skin (Fig. 5e). Briefly, the skin with size of 1 × 1 cm was stuck to a metal sheet by a double side glue and 4-HM solution was applied to the surface of skin. Fig. 5f shows the adhesive strength of 4-HM hydrogel compared to commercial tissue adhesives (Evicel and Coseal and fibrin glue). It could be concluded that the adhesive strength of 4-HM (39.6 ± 8.8 kPa) was significantly higher than that of two tissue adhesives. In addition, 4-HM hydrogel has competitive adhesive strength with other adhesive hydrogels such as MeTro/GelMA (45 kPa), GelMA (40 kPa) and Chitosan–poly(ethylene glycol)–tyramine (CPT) (17–97 kPa). The strong adhesion characteristics of the KaMA hydrogel could be related to various types of crosslinking process consisting of hydrogen bonding originated from the free hydroxyl groups [46], interconnection between hydrogel and tissue [47] as well as covalent interaction with radicals produced through crosslinking [48]. The visible-light crosslinked KaMA hydrogels provide numerous advantages compared to commercial adhesives, consisting of their favorable changeable properties depending on the polymer concentration and methacrylation degree as

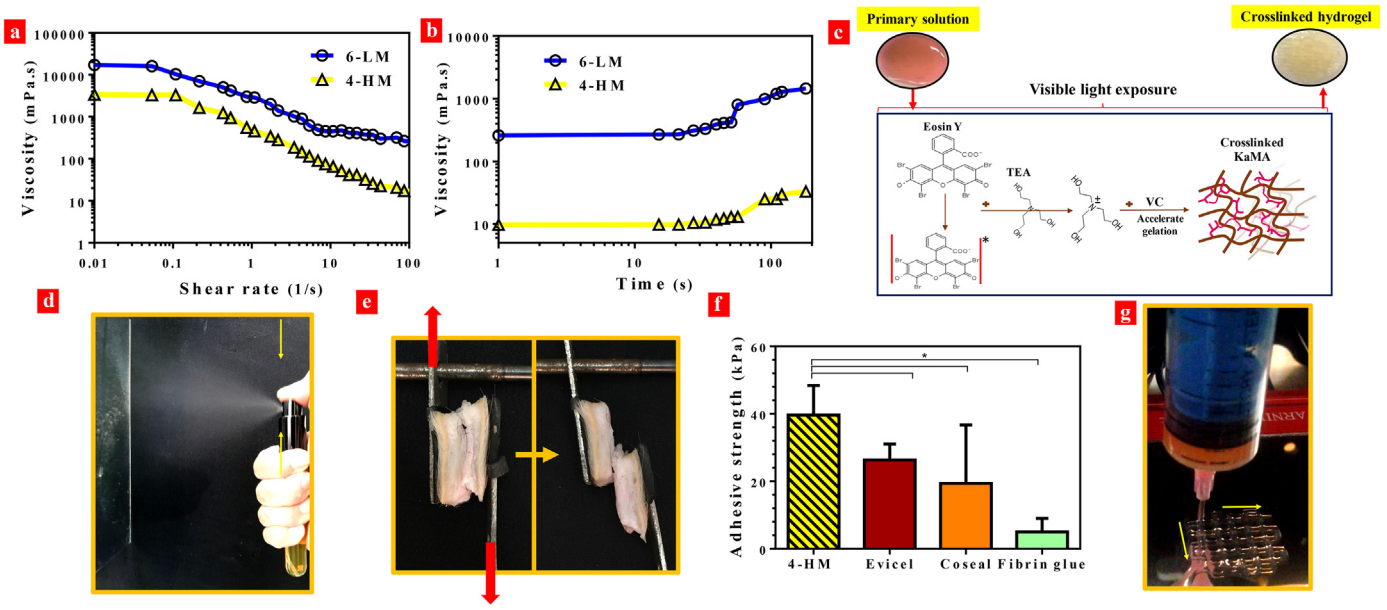

Fig. 5. a) Viscosity evaluation of 4-HM and 6-LM samples at different shear rates (1/s), b) gelation point of 4-HM and 6-LM hydrogels at the shear rate of 100 1/s. c) The schematic of visible-light crosslinking mechanism using Eosin Y, TEA and VC. d) The spray-ability of 4-HM primary solution. e) The pictures of adhesive strength system for 4-HM sample. f) The average adhesive strength of 4-HM hydrogel compared to three commercial types of adhesives. g) The print-ability of 6-LM primary solution.

well as greater adhesive strength to native tissue. In addition, the ability to easily modulate degradation rate, swelling ratio and mechanical properties of visible-light crosslinked KaMA hydrogel making it being a promising candidate for suture-less adhesives. In another word, according the viscoelastic properties (Fig. 5a), the 6-LM sample could be a more suitable material for injection and printing due to its higher viscosity at all shear rated than 4-HM. Also, the viscosity of this hydrogel decreased slightly with increasing shear rate, confirming the viscoelastic and shear tinning behavior which enable passing primary hydrogel solution throughout the needle. Thus, this hydrogel could be a proper choice in 3D bio-printing technology (Fig. 5g).

3.7. Protein adsorption evaluation

The role of various chemical and physical properties of the visible-light crosslinked KaMA hydrogel on the BSA adsorption was evaluated. BSA adsorption of hydrogel surfaces is the former stage of thrombosis on the surface of biomaterials. Generally, the enrichment of BSA adsorption indicates superior thrombotic characteristic [27]. In addition, BSA adsorption could significantly affect the cell function. In the body environment, biomaterial surfaces are immediately covered with protein from biological fluids influencing the cell adhesion, proliferation and migration [49] According to Fig. 6a, the amount of BSA adsorption on 4-HM hydrogel (9.4 ± 1.5 mg/g) was significantly greater than that of on the 6-LM sample (6.5 ± 0.9 mg/g), which might be due to difference in chain integration and structure stiffness. As discussed in Fig. 3a and d, elastic modulus and compressive modulus of 4-HM sample was lower than 6-LM hydrogel, leading to higher protein adsorption on 4-HM surface. This result was in agreement with the previous research of Wu et al. [50]. They discovered out that the significant BSA adsorption took place by lower stiff polymer. In contrast, stiffer polymer was less susceptible to fouling by protein adsorption.

3.8. Cell culture

Based on our above researches, 4-HM and 6-LM hydrogels revealed the optimized properties as sprayable/injectable hydrogels. Consequently, the cyto-compatibility of these hydrogels was investigated via in vitro viability, metabolic activity and proliferation of cells, via surface seeding. Primarily, live/dead kit was applied to evaluate the role of methacrylation degree and KaMA concentration on the viability of HeLa cells, during 5 days of culture. The live (green) and dead cells (red) were examining by fluorescence microscopy. Results revealed that living cell number (green) was more in 4-HM sample than live cells in 6-LM. Based on the live/dead images, the cell viability was evaluated regarding the number of live cells to total cells. Results showed cell viability of 4-HM sample (98 ± 2%) was higher than 6-LM one (81 ± 9%) (Fig. 6b–c). Similarly, the HeLa cell proliferation, estimated using DAPI staining (Fig. 6d) on 4-HM hydrogel was significantly higher than 6-LM sample. The cells were spread throughout the hydrogel surfaces. However, they severely agglomerated on some points of hydrogels, depending on the sample type. According to stained nucleus, the cell numbers were estimated after 1 and 5 days of culture (Fig. 6e). While the number of cells after a day of culture was not different on the two samples, it was significantly enhanced on 4-HM (521 ± 11 cells/mm^2) compared to 6-LM hydrogels (230 ± 15 cells/mm^2), after 5 days of culture. The more biocompatibility of 4-HM sample than 6-LM could be due to higher BSA adsorption on the 4-HM surface (Fig. 6a). Generally, the main production of a foreign material to cells is adsorbed proteins layer, in which the structure, composition and bioactivity of samples offer a biological interpretation of the underlying physicochemical characteristic [49]. Thus, the rate of protein adsorption plays a critical role in cell behavior on hydrogel surface. Adsorption the more content of protein aids cells to recognize hydrogel surface as a safe biointerface to proliferate and migrate.

The metabolic activity of cells on the two different samples was also investigated using MTT assay toward both HeLa and fibroblast cells, after 1, 3 and 5 days of culture (Fig. 6f–g). The substantial enhancement in cell survival during 5 days of culture on both 4-HM and 6-LM samples toward both kinds of cells was detected ($P < 0.05$), confirming that the samples were not cytotoxic and the cells proliferated over the incubation period. On the other hand, after 5 days of culture, cell survival on the 4-HM (145 ± 5%control) hydrogel was greater than that of on the 6-HM sample (131 ± 5%) toward HeLa cells, which might be due to different compressive and elastic modulus (Fig. 3a and d) of 4-HM and 6-LM hydrogels, leading to different protein adsorption on hydrogel surfaces. Similar trend was also detected toward fibroblast cells and the cell survival on the 4-HM (102 ± 7%control) specimen was significantly higher than that of on the 6-HM hydrogel (89 ± 6%) after 5 days of culture. Cells could compromise themselves straightforwardly with softer

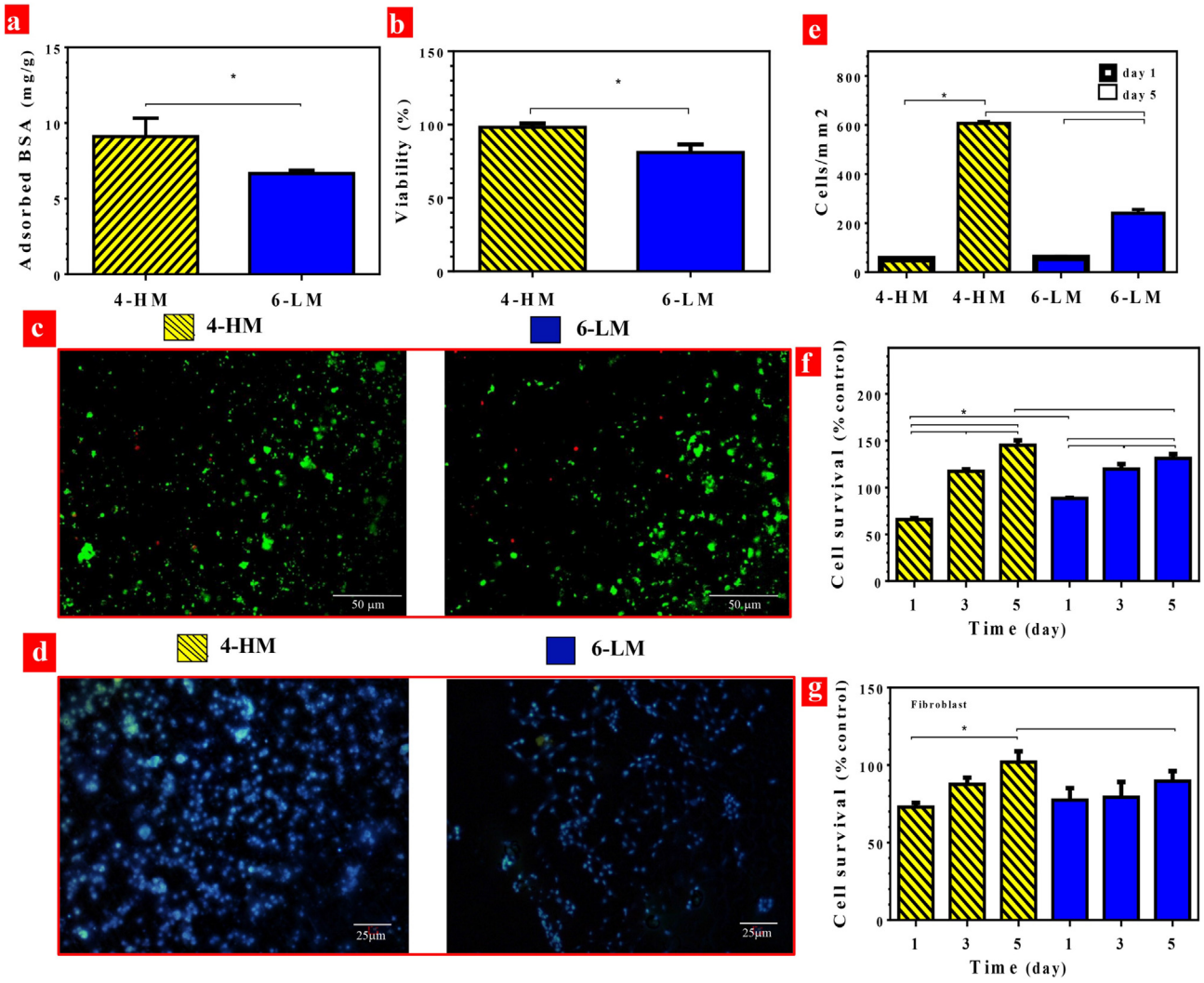

Fig. 6. a) Protein adsorption of the surface of 4-HM and 6-LM samples, b) cell viability calculated based on number of live cells, c) illustrative fluorescence images of live/dead assay at day 5 of culture. The cells were stained by Calcein AM (green) and EthDII (red), presented live and dead, respectively. d) Nuclei HeLa cells, cultured on 4-HM and 6-LM hydrogels for 5 days, were stained by DAPI (blue) after 5 days of culture. e) The proliferation of cells calculated based on DAPI staining. The survival of f) HeLa and g) fibroblast cells on various 4-HM and 6-LM hydrogels measured using MTT assays. The absorbance was normalized against the control (TCP) at each time interval (*$P < 0.05$).

environments than stiffer hydrogels [51]. Consequently, cells adapted more with 4-HM sample than 6-LM due to lower elastic and compressive modulus of 4-HM in comparison with 6-LM hydrogel. Similarly, Duan et al. [51] investigated on visible-light crosslinked HA hydrogels and reported that, the cells acclimated themselves more to softer hydrogel than stiffer one.

Our results established that the visible-light crosslinked KaMA hydrogels maintenance the attachment and proliferation of cells in vitro. Recently, Mihailia et al. [10] found that UV-crosslinked KaMA hydrogel was biocompatible and could promote cell proliferation compared to control. However, based on the cytotoxicity reports from Irgacure D-2959 photoinitiator [16,52] and harmful side effects of UV exposure [53], application of cell-compatible visible-light initiators in this study could be helpful to promote cell function. In addition, visible-light crosslinked KaMA hydrogel with significantly higher mechanical stiffness was developed. According to the efficient role of mechanical properties of the substrate on the protein adsorption and cell function [54], the role of polymer concentration and methacrylation degree of KaMA hydrogel was evaluated. Our results demonstrated that BSA adsorption and cell biocompatibility were higher on the softer hydrogel. So, 4-HM hydrogel with proper mechanical property and biocompatibility could be an outstanding biomaterial, in order to spray as a wound dressing in-situ.

4. Conclusions

In this study, a sprayable and injectable hydrogel based on visible-light crosslinked methacrylate-Kappa-carrageenan (KaMA) was introduced for in-situ soft tissue engineering. Results demonstrated that, higher methacrylation degree and more polymer concentration led to a denser crosslinked structure with stronger chain integration, less degradation rate, lower equivalent water content and mass swelling ratio. The adhesive strength of the KaMA hydrogel was also comparatively greater than commercially available tissue adhesives. Finally, the visible-light crosslinked KaMA hydrogels could maintenance attachment and proliferation of cells in vitro. Taken together, our results suggest the significant potential of visible-light crosslinked KaMA hydrogels for the engineering of soft tissues, suture-less adhesives and bio-printing applications without any harmful side effects which are associated with UV-light crosslinked hydrogel systems.

Acknowledgments

The author should have thanked from Iran National Science Foundation (INSF, Grant no. 94014204) and Isfahan University of Technology for financial support of this project.

Appendix A. Supplementary data

The Supporting information is composed of the hydrogel photos, FTIR spectrum of crosslinked 4-HM and 6-LM hydrogels and mechanical properties of UV-crosslinkable KaMA hydrogels. Supplementary data to this article can be found online at https://doi.org/10.1016/j.ijbiomac.2019.07.126.

References

[1] G.D. Nicodemus, S.J. Bryant, Cell encapsulation in biodegradable hydrogels for tissue engineering applications, Tissue Eng Part B Rev 14 (2) (2008) 149–165.
[2] K.Y. Lee, D.J. Mooney, Hydrogels for tissue engineering, Chemical Reveiw 101 (7) (2001) 1869–1880.
[3] N. Annabi, A. Tamayol, J.A. Uquillas, M. Akbari, L.E. Bertassoni, C. Cha, G. Camci-Unal, M.R. Dokmeci, N.A. Peppas, A. Khademhosseini, 25th anniversary article: rational design and applications of hydrogels in regenerative medicine, Adv. Mater. 26 (1) (2014) 85–124.
[4] H. Shin, B.D. Olsen, A. Khademhosseini, The mechanical properties and cytotoxicity of cell-laden double-network hydrogels based on photocrosslinkable gelatin and gellan gum biomacromolecules, Biomaterials 33 (11) (2012) 3143–3152.
[5] M.M. Stanton, J. Samitier, S. Sanchez, Bioprinting of 3D hydrogels, Lab Chip 15 (15) (2015) 3111–3115.
[6] A. Kumar, M. Jaiswal, Design and in vitro investigation of nanocomposite hydrogel based in situ spray dressing for chronic wounds and synthesis of silver nanoparticles using green chemistry, J. Appl. Polym. Sci. 133 (14) (2016) (n/a-n/a).
[7] A. Thakur, M.K. Jaiswal, C.W. Peak, J.K. Carrow, J. Gentry, A. Dolatshahi-Pirouz, A.K. Gaharwar, Injectable shear-thinning nanoengineered hydrogels for stem cell delivery, Nanoscale 8 (24) (2016) 12362–12372.
[8] J.-A. Yang, J. Yeom, B.W. Hwang, A.S. Hoffman, S.K. Hahn, In situ-forming injectable hydrogels for regenerative medicine, Prog. Polym. Sci. 39 (12) (2014) 1973–1986.
[9] D. Chouhan, T.U. Lohe, P.K. Samudrala, B.B. Mandal, In situ forming injectable silk fibroin hydrogel promotes skin regeneration in full thickness burn wounds, Adv Healthc Mater 7 (24) (2018) e1801092.
[10] S.M. Mihaila, A.K. Gaharwar, R.L. Reis, A.P. Marques, M.E. Gomes, A. Khademhosseini, Photocrosslinkable kappa-carrageenan hydrogels for tissue engineering applications, Adv Healthc Mater 2 (6) (2013) 895–907.
[11] N. Annabi, D. Rana, E. Shirzaei Sani, R. Portillo-Lara, J.L. Gifford, M.M. Fares, S.M. Mithieux, A.S. Weiss, Engineering a sprayable and elastic hydrogel adhesive with antimicrobial properties for wound healing, Biomaterials 139 (2017) 229–243.
[12] S.L. Fenn, R.A. Oldinski, Visible light crosslinking of methacrylated hyaluronan hydrogels for injectable tissue repair, J Biomed Mater Res B Appl Biomater 104 (6) (2016) 1229–1236.
[13] N.E. Fedorovich, M.H. Oudshoorn, D. van Geemen, W.E. Hennink, J. Alblas, W.J. Dhert, The effect of photopolymerization on stem cells embedded in hydrogels, Biomaterials 30 (3) (2009) 344–353.
[14] R. Prasad, S.K. Katiyar, Crosstalk among UV-induced inflammatory mediators, DNA damage and epigenetic regulators facilitates suppression of the immune system, Photochem. Photobiol. 93 (4) (2017) 930–936.
[15] K.A. Smeds, M.W. Grinstaff, Photocrosslinkable polysaccharides for *in situ* hydrogel formation, Journal of Biomedical Materials Research banner 55 (2) (2000) 254–255.
[16] C.S. Bahney, T.J. Lujan, C.W. Hsu, M. Bottlang, J.L. West, B. Johnstone, Visible light photoinitiation of mesenchymal stem cell-laden bioresponsive hydrogels, European cells and materials 22 (2016) 43–55.
[17] I. Noshadi, S. Hong, K.E. Sullivan, E. Shirzaei Sani, R. Portillo-Lara, A. Tamayol, S.R. Shin, A.E. Gao, W.L. Stoppel, L.D. Black, III, A. Khademhosseini, N. Annabi, In vitro and in vivo analysis of visible light crosslinkable gelatin methacryloyl (GelMA) hydrogels, Biomater Sci 5 (10) (2017) 2093–2105.
[18] G. Lokhande, J.K. Carrow, T. Thakur, J.R. Xavier, M. Parani, K.J. Bayless, A.K. Gaharwar, Nanoengineered injectable hydrogels from kappa-carrageenan and two-dimensional nanosilicates for wound healing application, Acta Biomater. 70 (2018) 35–47.
[19] Y.-M. Lim, H.-J. Gwon, J.-H. Choi, J. Shin, Y.-C. Nho, S.I. Jeong, M.S. Chong, Y.-M. Lee, I.K. Kwon, S.E. Kim, Preparation and biocompatibility study of gelatin/kappa-carrageenan scaffolds, Macromol. Res. 18 (1) (2010) 29–34.
[20] S. Distantina, R. Rochmadi, M. Fahrurrozi, W. Wiratni, Preparation and characterization of glutaraldehyde-crosslinked kappa carrageenan hydrogel, Engineering Journal 17 (3) (2013) 57–66.
[21] V.D. Prajapati, P.M. Maheriya, G.K. Jani, H.K. Solanki, Carrageenan: a natural seaweed polysaccharide and its applications, Carbohydr. Polym. 105 (2014) 97–112.
[22] A.A. Oun, J.-W. Rhim, Carrageenan-based hydrogels and films: effect of ZnO and CuO nanoparticles on the physical, mechanical, and antimicrobial properties, Food Hydrocoll. 67 (2017) 45–53.
[23] S. Azizi, R. Mohamad, R. Abdul Rahim, R. Mohammadinejad, A. Bin Ariff, Hydrogel beads bio-nanocomposite based on Kappa-Carrageenan and green synthesized silver nanoparticles for biomedical applications, Int J Biol Macromol 104(Pt A) (2017) 423–431.
[24] C. Esmaeili, L.Y. Heng, C.P. Chiang, Z.A. Rashid, E. Safitri, R.S.P. Malon Marugan, A DNA biosensor based on kappa-carrageenan-polypyrrole-gold nanoparticles composite for gender determination of Arowana fish (Scleropages formosus), Sensors Actuators B Chem. 242 (2017) 616–624.
[25] G. Bardajee, Z. Hooshyar, F. Rastgo, Kappa carrageenan-g-poly (acrylic acid)/SPION nanocomposite as a novel stimuli-sensitive drug delivery system, Colloid Polym. Sci. 291 (12) (2013) 2791–2803.
[26] H. Mokhtari, M. Kharaziha, F. Karimzadeh, S. Tavakoli, An injectable mechanically robust hydrogel of Kappa-carrageenan-dopamine functionalized graphene oxide for promoting cell growth, Carbohydr. Polym. 214 (2019) 234–249.
[27] N. Golafshan, R. Rezahasani, M. Tarkesh Esfahani, M. Kharaziha, S.N. Khorasani, Nanohybrid hydrogels of laponite: PVA-alginate as a potential wound healing material, Carbohydr. Polym. 176 (2017) 392–401.
[28] H. Mokhtari, Z. Ghasemi, M. Kharaziha, F. Karimzadeh, F. Alihosseini, Chitosan-58S bioactive glass nanocomposite coatings on TiO2 nanotube: structural and biological properties, Appl. Surf. Sci. 441 (2018) 138–149.
[29] N.N. Mobarak, N. Ramli, A. Ahmad, M.Y.A. Rahman, Chemical interaction and conductivity of carboxymethyl κ-carrageenan based green polymer electrolyte, Solid State Ionics 224 (2012) 51–57.
[30] L.V. Abad, S. Saiki, N. Nagasawa, H. Kudo, Y. Katsumura, A.M. De La Rosa, NMR analysis of fractionated irradiated κ-carrageenan oligomers as plant growth promoter, Radiat. Phys. Chem. 80 (9) (2011) 977–982.
[31] Y. Guo, T. Yuan, Z. Xiao, P. Tang, Y. Xiao, Y. Fan, X. Zhang, Hydrogels of collagen/chondroitin sulfate/hyaluronan interpenetrating polymer network for cartilage tissue engineering, J Mater Sci Mater Med 23 (9) (2012) 2267–2279.
[32] Y. Shi, D. Xiong, Microstructure and friction properties of PVA/PVP hydrogels for articular cartilage repair as function of polymerization degree and polymer concentration, Wear 305 (1–2) (2013) 280–285.
[33] N.A. Peppas, J.Z. Hilt, A. Khademhosseini, R. Langer, Hydrogels in biology and medicine: from molecular principles to bionanotechnology, Adv. Mater. 18 (11) (2006) 1345–1360.
[34] N. Annabi, J.W. Nichol, X. Zhong, C. Ji, S. Koshy, A. Khademhosseini, F. Dehghani, Controlling the porosity and microarchitecture of hydrogels for tissue engineering, Tissue Engineering: Part B 16 (2010) 371–383.
[35] M. Lee, B.M. Wu, J.C. Dunn, Effect of scaffold architecture and pore size on smooth muscle cell growth, J. Biomed. Mater. Res. A 87 (4) (2008) 1010–1016.
[36] F. Flament, G. Francois, H. Qiu, C. Ye, T. Hanaya, D. Batisse, S. Cointereau-Chardon, M.D. Seixas, S.E. Dal Belo, R. Bazin, Facial skin pores: a multiethnic study, Clin. Cosmet. Investig. Dermatol. 8 (2015) 85–93.
[37] J.W. Nichol, S.T. Koshy, H. Bae, C.M. Hwang, S. Yamanlar, A. Khademhosseini, Cell-laden microengineered gelatin methacrylate hydrogels, Biomaterials 31 (21) (2010) 5536–5544.
[38] N. Bhardwaj, D. Chouhan, B.B. Mandal, 3D Functional Scaffolds for Skin Tissue Engineering, 2018 345–365.
[39] E.J. Chen, J. Novakofski, W.K. Jenkins, W.D. O'Brien, Young's modulus measurements of soft tissues with application to elasticity imaging, IEEE Trans. Ultrason. Ferroelectr. Freq. Control 43 (1) (1996).
[40] S. Kim, C. Chu, Pore structure analysis of swollen dextran-methacrylate hydrogels by SEM and mercury intrusion porosimetry, Journal of Biomedical Materials Research banner 53 (3) (2000) 258–266.
[41] N. Rhein-Knudsen, M.T. Ale, A.S. Meyer, Seaweed hydrocolloid production: an update on enzyme assisted extraction and modification technologies, Mar Drugs 13 (6) (2015) 3340–3359.
[42] X. Hu, L. Ma, C. Wang, C. Gao, Gelatin hydrogel prepared by photo-initiated polymerization and loaded with TGF-beta1 for cartilage tissue engineering, Macromol. Biosci. 9 (12) (2009) 1194–1201.
[43] F. Ganji, M.J. Abdekhodaie, A. Ramazani, S.A, Gelation time and degradation rate of chitosan-based injectable hydrogel, J. Sol-Gel Sci. Technol. 42 (1) (2007) 47–53.
[44] L. Durand, N. Habran, C. Denisà, L. Meuldersà, V. Henschel, K. Amighi, Influence of different parameters on droplet size and size distribution of sprayable sunscreen emulsions with high concentration of UV-filters, Int. J. Cosmet. Sci. 29 (2007) 461–471.
[45] B.J. Kim, D.X. Oh, S. Kim, J.H. Seo, D.S. Hwang, A. Masic, D.K. Han, H.J. Cha, Mussel-mimetic protein-based adhesive hydrogel, Biomacromolecules 15 (5) (2014) 1579–1585.
[46] J.D. Smart, The basics and underlying mechanisms of mucoadhesion, Adv. Drug Deliv. Rev. 57 (11) (2005) 1556–1568.
[47] N. Lang, M.J. Pereira, Y. Lee, I. Friehs, N.V. Vasilyev, E.N. Feins, K. Ablasser, E.D. O'Cearbhaill, C. Xu, A. Fabozzo, R. Padera, S. Wasserman, F. Freudenthal, L.S. Ferreira, R. Langer, J.M. Karp, P.J. del Nido, A blood-resistant surgical glue for minimally invasive repair of vessels and heart defects, Sci. Transl. Med. 6 (218) (2014) 218ra6.
[48] M. Yao, A. Yaroslavsky, F.P. Henry, R.W. Redmond, I.E. Kochevar, Phototoxicity is not associated with photochemical tissue bonding of skin, Lasers Surg. Med. 42 (2) (2010) 123–131.
[49] C.J. Wilson, R.E. Clegg, D.I. Leavesley, M.J. Pearcy, Mediation of biomaterial–cell interactions by adsorbed proteins: a review, Tissue Eng. 11 (2005).
[50] B. Wu, G. Liu, G. Zhang, V.S. Craig, Stiff chains inhibit and flexible chains promote protein adsorption to polyelectrolyte multilayers, Soft Matter 10 (21) (2014) 3806–3816.
[51] B. Duan, L.A. Hockaday, E. Kapetanovic, K.H. Kang, J.T. Butcher, Stiffness and adhesivity control aortic valve interstitial cell behavior within hyaluronic acid based hydrogels, Acta Biomater. 9 (8) (2013) 7640–7650.
[52] N.S. Allen, Photoinitiators for UV and visible curing of coatings mechanisms and properties, J. Photochem. Photobiol. A Chem. 100 (1996) 101–107.
[53] D.C. Birdsell, P.J. Bannon, R.B. Webb, Harmful effects of near-ultraviolet radiation used for polymerization of a sealant and a composite resin, J. Am. Dent. Assoc. 94 (2) (1977) 311–314.
[54] A.M. Kloxin, C.J. Kloxin, C.N. Bowman, K.S. Anseth, Mechanical properties of cellularly responsive hydrogels and their experimental determination, Adv. Mater. 22 (31) (2010) 3484–3494.